Proline-rich tyrosine kinase 2 regulates osteoprogenitor cells and bone formation, and offers an anabolic treatment approach for osteoporosis

Leonard Buckbinder*†, David T. Crawford*, Hong Qi*, Hua Zhu Ke*‡, Lisa M. Olson§¶, Kelly R. Long§, Peter C. Bonnette*, Amy P. Baumann*, John E. Hambor*, William A. Grasser III*, Lydia C. Pan*, Thomas A. Owen*, Michael J. Luzzio*, Catherine A. Hulford*, David F. Gebhard*, Vishwas M. Paralkar*, Hollis A. Simmons*, John C. Kath*‖, W. Gregory Roberts*, Steven L. Smock*, Angel Guzman-Perez*, Thomas A. Brown*, and Mei Li*

*Pfizer Global Research and Development, Groton, CT 06340; and §Pfizer Global Research and Development, Chesterfield, MO 63198

Edited by Owen N. Witte, University of California, Los Angeles, CA, and approved April 18, 2007 (received for review February 16, 2007)

Bone is accrued and maintained primarily through the coupled actions of bone-forming osteoblasts and bone-resorbing osteoclasts. Cumulative *in vitro* studies indicated that proline-rich tyrosine kinase 2 (PYK2) is a positive mediator of osteoclast function and activity. However, our investigation of PYK2−/− mice did not reveal evidence supporting an essential function for PYK2 in osteoclasts either *in vivo* or in culture. We find that PYK2−/− mice have high bone mass resulting from an unexpected increase in bone formation. Consistent with the *in vivo* findings, mouse bone marrow cultures show that PYK2 deficiency enhances differentiation and activity of osteoprogenitor cells, as does expressing a PYK2-specific short hairpin RNA or dominantly interfering proteins in human mesenchymal stem cells. Furthermore, the daily administration of a small-molecule PYK2 inhibitor increases bone formation and protects against bone loss in ovariectomized rats, an established preclinical model of postmenopausal osteoporosis. In summary, we find that PYK2 regulates the differentiation of early osteoprogenitor cells across species and that inhibitors of the PYK2 have potential as a bone anabolic approach for the treatment of osteoporosis.

human mesenchymal stem cell | osteoclast | osteoblast

Proline-rich tyrosine kinase 2 (PYK2) and focal adhesion kinase (FAK) are nonreceptor tyrosine kinases, and together they constitute the focal adhesion kinase subfamily (1). Unlike FAK, PYK2 expression is relatively restricted, with highest levels in the brain and the hematopoietic system. PYK2−/− mice have been described previously and appear normally developed (2, 3). Characterization of the immune system of PYK2−/− animals revealed the absence of marginal zone B cells along and abnormal T cell-independent type II responses (2), as well as altered macrophage morphology, adhesion, and migration (3).

Although PYK2 is expressed in both bone-forming osteoblasts and bone-resorbing osteoclasts, the skeletal phenotype of PYK2−/− mice has not been described. *In vitro* studies pointed to a positive role for PYK2 in osteoclast maturation and bone resorption. PYK2 localizes to the podosomes of osteoclasts (4), and, upon integrin binding, cell attachment, and actin ring formation, PYK2 associates with a variety of proteins including $p130^{CAS}$ (5), Src (4), Cbl (6), integrins (4), gelsolin (7), and paxillin (8). Antisense depletion of PYK2 (9), but not the expression of a kinase inactive dominant negative mutant (10), blocked osteoclast spreading and bone resorption, indicating that PYK2 catalytic activity may be dispensable. The *in vitro* effects of bone anabolic stimuli suggested that PYK2 might have a positive role in osteoblasts as well. Treatment of osteoblast cells with fluoroaluminate led to increased PYK2 autophosphorylation, Src association, and kinase activity (11) and was associated with increased cell attachment and spreading (12). Likewise, in an anabolic model of mechanical loading, PYK2 autophosphorylation and kinase activity were stimulated in osteoblast-like cells after mechanical strain (13, 14). In this article we elucidate the function of PYK2 in bone using PYK2−/− mice and bone marrow cultures derived therefrom, expression of PYK2 short hairpin RNA and interfering proteins in human mesenchymal stem cells (hMSCs), and a pharmacological inhibitor in a preclinical model of osteoporosis.

Results

The High Bone Mass of PYK2−/− Mice Results from Increased Bone Formation. We began by characterizing the skeletal phenotype of adult female PYK2−/− mice and WT controls at ≈18 weeks of age. The PYK2−/− mice we have studied were extensively backcrossed to C57BL/6, and their derivation has been reported (3, 15). In agreement with previous findings, the PYK2−/− mice were normal in appearance and in body weight (data not shown). Radiographic and microcomputed tomography (μCT) analysis of the femur (Fig. 1*A* and *B*) and vertebrae (Fig. 1*C*) showed that PYK2−/− animals had bones of normal shape and size, but with an apparent increase in bone mass. Quantitative μCT analyses demonstrated a significant increase in volumetric bone mineral density in both the distal femur and lumbar vertebrae (338% and 164% of controls, respectively) (Fig. 1*D*). The trabecular number and thickness were significantly increased in the distal femur of PYK2−/− animals relative to WT controls (Fig. 1 *E* and *F*) (248% and 178% of controls, respectively), resulting in a dramatic increase in trabecular bone volume (+595% of controls) (Fig. 1*G*). A similar response was seen in the lumbar vertebrae from PYK2−/− mice, with trabecular number, trabecular thickness, and bone volume per tissue volume increased to 151%, 141%, and 225% of controls, respectively (Fig. 1 *E*–*G*). These data demonstrated a high bone mass phenotype with improved

Author contributions: L.B., H.Z.K., L.M.O., J.E.H., V.M.P., A.G.-P., T.A.B., and M.L. designed research; D.T.C., H.Q., K.R.L., P.C.B., A.P.B., W.A.G., L.C.P., T.A.O., and H.A.S. performed research; M.J.L., C.A.H., D.F.G., J.C.K., W.G.R., and S.L.S. contributed new reagents/analytic tools; and L.B. wrote the paper.

The authors declare no conflict of interest.

This article is a PNAS Direct Submission.

Freely available online through the PNAS open access option.

Abbreviations: hMSC, human mesenchymal stem cell; μCT, microcomputed tomography; OVX, ovariectomized; PYK2, proline-rich tyrosine kinase 2; TRAP, tartrate-resistant acid phosphatase; SH, short hairpin RNA; EE, ethynyl estradiol.

†To whom correspondence should be addressed. E-mail: leonard.buckbinder@pfizer.com.

‡Present address: Amgen, Inc., 1 Amgen Center Drive, Thousand Oaks, CA 91320.

¶Present address: Abbott Bioresearch Center, 100 Research Drive, Worcester, MA 01605.

‖Present address: Pfizer Global Research and Development, 10646 Science Center Drive, La Jolla, CA 92121.

This article contains supporting information online at www.pnas.org/cgi/content/full/0701421104/DC1.

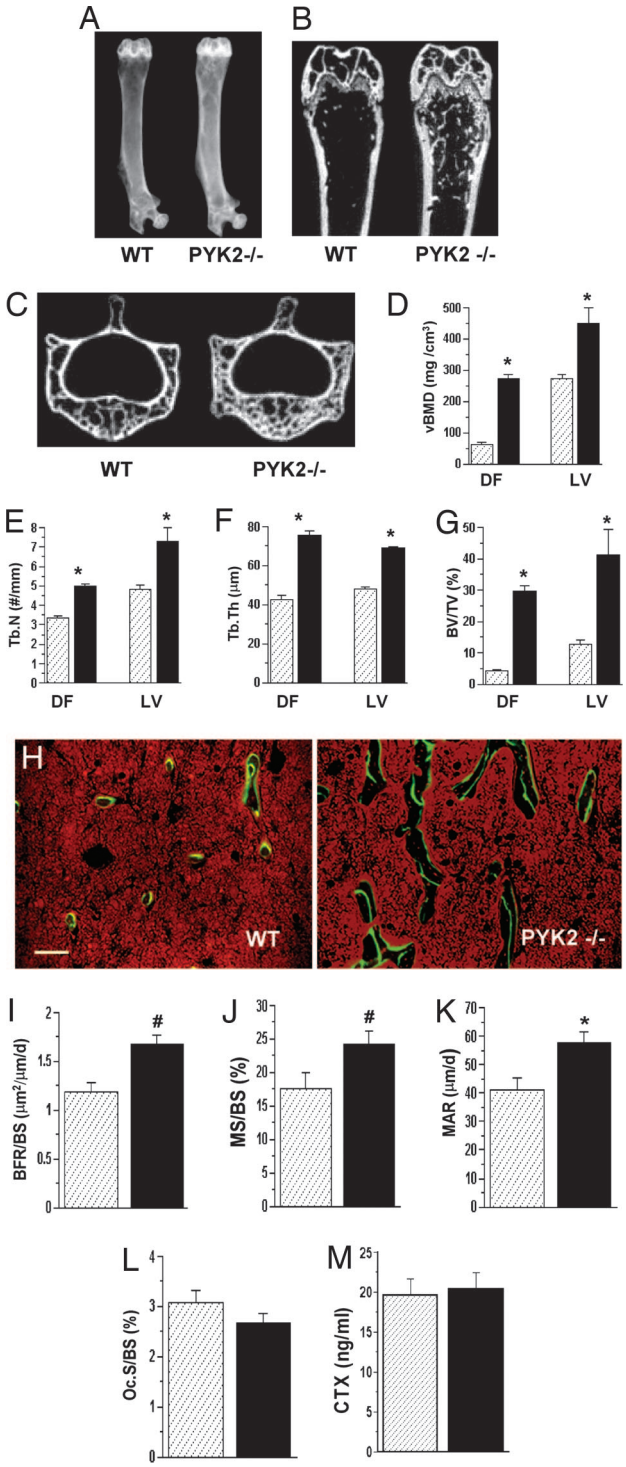

Fig. 1. Bone mass and bone formation are dramatically increased in adult PYK2−/− mice at 18 weeks of age. (*A*) Radiography of isolated femurs from female WT control and PYK2−/− mice. (*B* and *C*) μCT images of the distal femur (*B*) and second lumbar vertebrae (*C*) of WT control and PYK2−/− mice. (*D–G*) Quantitative analysis of μCT images of the distal femur and second lumbar vertebrae from WT control mice and PYK2−/− mice. (*D*) Volumetric bone mineral density (vBMD) in WT control (hatched bars) and PYK2−/− mice (black bars). (*E*) Trabecular number (Tb.N). (*F*) Trabecular thickness (Tb.Th). (*G*) Cancellous bone volume per tissue volume. (*H*) Calcein labeling of cancellous bone in proximal tibia (green) was visualized by fluorescence micrography, with Villanueva bone counterstain (red background). (Scale bar: 100 μm.) (*I–L*) Dynamic histomorphometry of cancellous bone. Bone surface referent bone formation rate (BFR/BS) (*I*), mineralizing surface per bone surface (MS/BS) (*J*), and mineral apposition rate (*K*) are significantly increased in PYK2−/− animals. (*L*) Osteoclast surface (Oc.S/BS). (*M*) Serum CTX concentration. All data are presented as means ± SEM; n = 12–14 animals per genotype. *, $P < 0.01$; #, $P < 0.05$. Significance was determined by ANOVA followed by Fisher's protected least significant difference test to compare differences among groups. $P < 0.05$ was considered significant.

microstructure in the PYK2−/− mice, indicating that there is an inhibitory effect of PYK2 on bone mass.

To gain insight at the tissue level into the mechanism responsible for the increased bone mass in PYK2−/− animals, dynamic histomorphometry of the proximal tibia metaphysis was performed. Quantitation of fluorochrome label, which is incorporated into actively mineralizing bone as visualized in representative tissue sections in Fig. 1*H*, indicated a highly significant increase in the bone formation rate per bone surface for PYK2−/− animals (139% of controls) (Fig. 1*I*), resulting from both increased mineralizing surface per bone surface and the mineral apposition rate (137% and 142% of controls, respectively) (Fig. 1 *J* and *K*). These data showed that PYK2 regulates both osteoblastogenesis and osteoblast activity. The effect of PYK2 on bone resorption was also examined. Given that PYK2 appeared to have an important function in osteoclast adhesion and activity *in vitro* (4, 6, 9, 10), we were surprised to find no significant difference in osteoclast surface per unit bone surface in PYK2−/− mice (Fig. 1*L*). Furthermore, levels of serum CTX (collagen I carboxyl-terminal telopeptide fragments), a type I collagen degradation product that reflects osteoclast activity and bone resorption, were similar between WT and PYK2−/− animals (Fig. 1*M*). These analyses show that the augmented bone mass observed in the PYK2−/− mice results primarily from increased bone formation.

Marrow-Derived Osteoclasts from PYK2−/− Mice Are Similar to WT Controls. Because cumulative *in vitro* studies suggested a function of PYK2 in osteoclasts that was not obvious from our *in vivo* analysis, we examined osteoclast differentiation in bone marrow cultures. When equal numbers of bone marrow cells from WT and PYK2−/− animals were differentiated in the presence of osteoprotegerin ligand and macrophage colony-stimulating factor, the total numbers of multinucleated, tartrate-resistant acid phosphatase-positive (TRAP+) cells were found not to be significantly different (Fig. 2 *A* and *B*). The marrow-derived PYK2−/− and WT osteoclasts also resorbed the same total area on calcium phosphate-coated discs (Fig. 2 *C* and *D*). Previous studies identified a positive role for PYK2 in the function of mature osteoclasts as well as in osteoclastogenesis in osteoblast cocultures (4–6, 9, 10) that was not evident in our study of osteoclasts differentiated from bone marrow cultures of PYK2−/− mice using defined media (Fig. 2). Although these differences could be of relevance to explaining these disparate results, there is consistency between our *in vitro* and *in vivo* findings. Thus, we conclude that osteoclasts derived from PYK2−/− mice are similar in number and activity to WT mice.

PYK2 Is an Inhibitor of Osteoprogenitor Stem Cells. Because the high bone mass of PYK2−/− mice did not appear to result from osteoclast impairment, we investigated whether PYK2 may regulate osteogenesis using bone marrow cells derived from WT and PYK2−/− mice. Equal numbers of bone marrow cells were divided into replicate dishes and cultured in osteogenic media for up to 22 days. Cultures from PYK2−/− animals showed significantly elevated alkaline phosphatase activity, an early marker of osteoblast differentiation (Fig. 3*A*). Fluorochrome label incorporation showed that marrow cultures from PYK2−/− animals mineralized to a greater degree than control cultures (Fig. 3*B*). These results suggested that PYK2 may be a

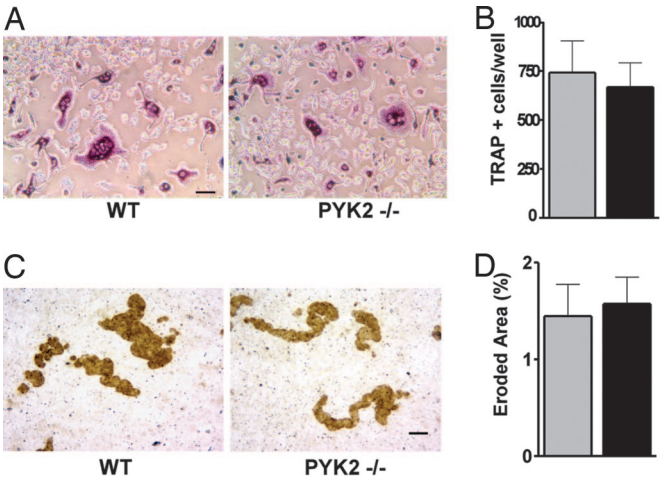

Fig. 2. Normal osteoclastogenesis in bone marrow cultures from PYK2−/− mice. (*A*) Equal numbers of cells from tibial bone marrow isolated from WT control and PYK2−/− animals were plated and cultured in media supplemented with osteoprotegerin ligand and macrophage colony-stimulating factor for 4 days. Cells were fixed and stained for the presence of TRAP expression (TRAP+ cells are stained purple). (Scale bar: 50 μm.) (*B*) Multinucleated TRAP+ cells were counted from control (gray bar) and PYK2−/− (black bar) cultures ($n = 4$ wells). (*C*) Bone marrow-derived osteoclast cultures were grown on calcium phosphate-coated discs to assess mineral resorptive activity (osteoclast eroded surface appears brown). (Scale bar: 50 μm.) (*D*) Image analysis software was used to calculate the total disc eroded area in WT (gray bar) and PYK2−/− (black bar) cultures ($n = 6$ discs).

negative regulator of osteoprogenitor cells. We also examined the differentiation potential of osteoblastic cells isolated from newborn calvaria, which comprise a more differentiated osteoblast population. In contrast to the marrow cultures, there was no consistent difference in alkaline phosphatase expression between the WT control and PYK2−/− cultures [supporting information (SI) Fig. 6].

Together, the marrow and calvarial culture results suggested that PYK2 might function at an early phase in osteoprogenitor cell differentiation. Thus, we used hMSCs as a model to further study the role of PYK2 in osteogenesis. We inhibited PYK2 by two different approaches: (*i*) adenoviral delivery of a PYK2-targeted short hairpin RNA (SH), and (*ii*) expression of dominantly interfering proteins, a catalytically inactive PYK2 mutant K457A (KD), and a C-terminal protein splice variant, PRNK (16, 17) (SI Fig. 7*A*). Replicate cultures of hMSCs infected with the

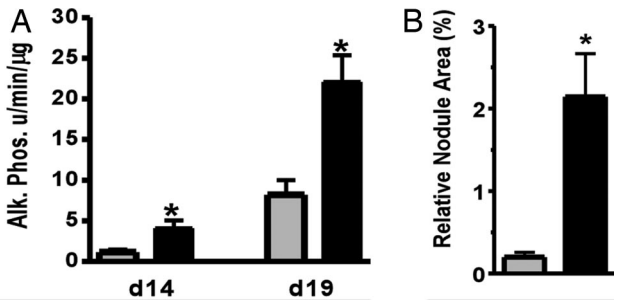

Fig. 3. Osteogenesis is enhanced in bone marrow cultures from PYK2−/− mice. Equal numbers of bone marrow cells from WT (gray bars) and PYK2−/− (black bars) animals were cultured in osteogenic differentiation medium. Cell lysates were analyzed for alkaline phosphatase activity on days 14 and 19 (*A*) or assessed for mineralized area by quantitative fluorography of calcein labeled nodules on day 22 (*B*). All data are presented as means ± SEM. *, $P <$ 0.01. Significance was determined by unpaired *t* test to compare differences between the indicated groups. $P < 0.05$ was considered significant.

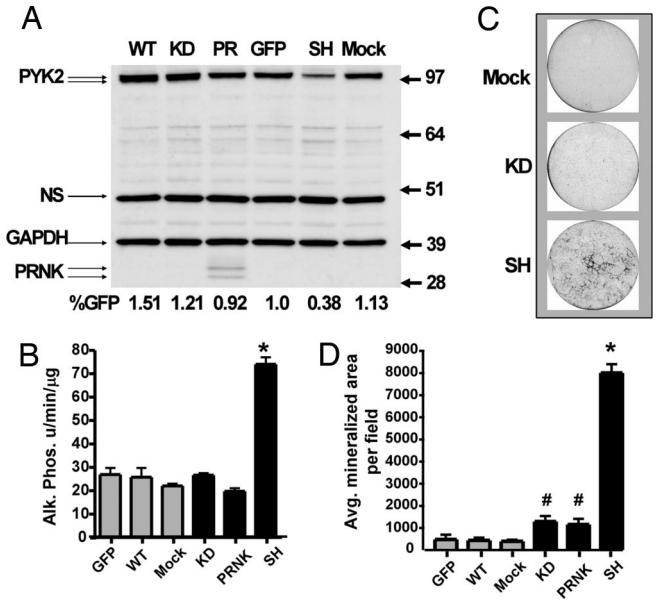

Fig. 4. PYK2 short hairpin RNA and dominantly interfering proteins enhance the osteogenesis of hMSC cultures. hMSCs plated in basal growth medium were infected with adenoviruses expressing a GFP control, WT PYK2, a kinase-dead PYK2 mutant (KD), a dominant interfering PYK2 splice variant (PRNK), SH, or uninfected (mock) control as indicated (see *Methods* and SI Fig. 7*A*). (*A*) Western blot analysis of protein extracts prepared 7 days after infection and codeveloped with monoclonal antibodies recognizing the carboxyl terminus of PYK2 and a GAPDH loading control. The positions of molecular mass markers are indicated in kilodaltons (on the right), with protein products designated on the left (NS, nonspecific). Quantitative image analysis of the full-length PYK2 doublet was normalized to GAPDH and expressed relative to PYK2 present in the GFP control sample (% GFP, at the bottom). (*B*) Alkaline phosphatase activity was measured on day 10. PYK2 SH was significantly different from the GFP controls ($n = 3$). (*C*) A negative well image of calcein-labeled hMSC bone nodules taken by fluorescent micrography as indicated. (*D*) Calcein-labeled bone nodule area was quantified by image analysis. SH, KD, and PRNK were significantly different from the GFP control ($n = 3$). All data are presented as means ± SEM. Significance was determined by unpaired *t* test to compare differences between the indicated groups. $P < 0.05$ was considered significant (*, $P < 0.01$; #, $P < 0.05$).

aforementioned adenovirus constructs or additional controls (GFP, WT PYK2, or mock-infected) were grown in osteogenic media and analyzed for PYK2 protein expression, alkaline phosphatase activity, and mineralized bone nodule formation. Fig. 4*A* shows Western blot analysis from samples prepared 7 days after infection. Compared with the GFP control there was a modest increase in PYK2 protein with the WT-expressing (≈50%) and KD-expressing (20%) viruses. In PRNK-expressing cells we detected an appropriately sized protein doublet of ≈30 kDa, which may arise from heterogeneous phosphorylation of the known Y881 site. The modest level of PYK2 transexpression is consistent with previous observations that PYK2 levels are tolerated within a limited range (ref. 16 and data not shown). Importantly, the SH-expressing virus resulted in >60% knockdown of the endogenous PYK2 protein.

Replicate cell cultures were analyzed for alkaline phosphatase activity between days 2 and 16. The SH-expressing cultures were distinguished from all others by day 4 and showed a significant ≈2.5-fold elevation in alkaline phosphatase activity at day 10 (Fig. 4*B* and SI Fig. 7*B*), whereas the alkaline phosphatase activity was similar to GFP and mock controls for all other groups. On day 16 the cultures were fixed and bone nodule formation was determined. The mineralized area increased significantly, >2-fold in cultures expressing both KD and PRNK, and a remarkable 16-fold in SH-expressing cultures (Fig. 4 *C* and

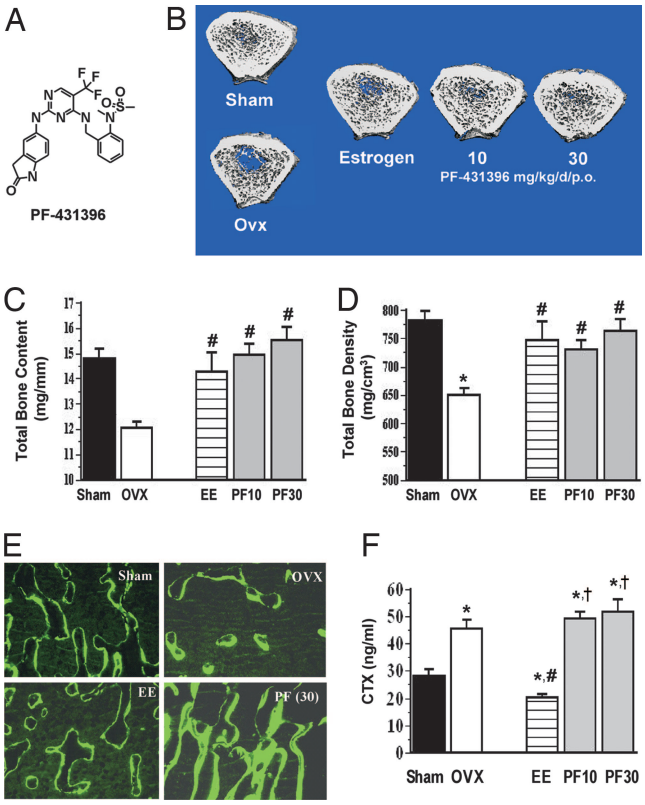

Fig. 5. A PYK2 inhibitor increases bone formation and blocks bone loss in ovariectomized (OVX) rats. (*A*) The chemical structure of PF-431396, a PYK2 inhibitor. (*B*) Representative three-dimensional μCT images of the distal femur from the indicated treatment groups. (*C*) Peripheral quantitative computed tomography (pQCT) analysis of total bone content: sham control (black bar), OVX vehicle (open bar), ethynyl estradiol (EE) (hatched bar), and PF-431396 treatment (gray bars). (*D*) pQCT analysis of total bone density (groups as in *C*). (*E*) Histomorphometric analysis of cancellous bone from the proximal tibia. Shown are fluorescent micrographs of the indicated treatment groups (see Table 1 for quantitative results). (*F*) Serum CTX levels corresponding to the indicated treatment groups (as in *C*). All data are presented as means ± SEM; $n = 10$ animals per treatment group. *, $P < 0.05$ vs. sham control; #, $P < 0.05$ vs. OVX; +, $P < 0.05$ vs. EE. Significance was determined by ANOVA followed by Fisher's protected least significant difference test to compare differences between groups. $P < 0.05$ was considered significant.

D). Similar effects on osteogenesis were obtained by transfection of hMSCs with independent PYK2 siRNA (SI Fig. 8 *A* and *B*). These findings indicate that PYK2 is a cell-autonomous inhibitor of hMSC osteogenic differentiation, and this is consistent with our findings *in vivo*.

A PYK2 Inhibitor Increases Bone Formation and Prevents Bone Loss in OVX Rats. We next tested whether the pharmacological modulation of PYK2 activity may impact bone mass in the OVX rats, an established preclinical disease model of postmenopausal osteoporosis, using PF-431396, a potent pyrimidine-based PYK2 inhibitor having an IC_{50} of 31 nM against the recombinant PYK2 enzyme (Fig. 5*A* and *SI Methods*). Four-month-old OVX rats were treated daily for 28 days with vehicle, PF-431396 (10 and 30 mg/kg), or EE, an antiresorptive agent. Pharmacokinetic studies indicated that the free plasma concentration of PF-431396 covers the PYK2 IC_{50} for at least 8 h at the high dose (data not shown). As shown in μCT images of the distal femur metaphases (Fig. 5*B*), vehicle-treated OVX rats had less trabecular bone mass than the sham controls. Both EE and PF-431396 counteracted OVX-induced bone loss, completely preserving total bone content and total bone density (Fig. 5 *C* and *D*). In agreement with previous studies, the vehicle-treated OVX rats exhibited high bone turnover characterized by increased bone formation (mineralizing surface per bone surface and bone formation rate per bone surface) and bone resorption (osteoclast surface and serum CTX) compared with sham controls (Table 1 and Fig. 5 *E* and *F*). Treatment of OVX rats with EE suppressed the high bone turnover as evidenced by decreased bone resorption and formation relative to vehicle treatment. In contrast to EE, both doses of PF-431396 significantly increased bone formation rate, which was accompanied by an elevation in mineralizing surface and mineral apposition rate (Table 1 and Fig. 5*E*), suggesting that PF-431396 promotes osteoblast recruitment and activity. Consistent with this, PF-431396 increased alkaline phosphatase activity in 7-day hMSC cultures (P.C.B. and L.B., data not shown). Although high-dose PF-431396 decreased osteoclast surface (a referent parameter of bone resorption) at the proximal tibia, it did not alter serum CTX (a systemic biomarker of bone resorption) at either dose after both 2 weeks (data not shown) and 4 weeks (Fig. 5*F*) of treatment. These results showed that PF-431396, a potent PYK2 inhibitor, prevents bone loss induced by estrogen deficiency in rats primarily by stimulating bone formation, providing independent pharmacological confirmation for the function of PYK2 in regulating bone formation.

Discussion

In this study we show that PYK2 is a cell-autonomous inhibitor of the differentiation of osteoprogenitor cells. This contributes to significantly elevated bone mass and bone formation in PYK2−/− mice. We emphasize that PYK2 is not required for the normal development of the skeleton and is therefore one of a handful of genes known to regulate adult bone mass principally through an effect on bone formation. This result was unexpected, because previously described *in vitro* studies focused on PYK2 in osteoclasts. Conversely, we found little difference between osteoclasts derived from adult PYK2−/− and control animals either *in vitro* or *in vivo* (Figs. 1 *L* and *M* and 2), nor did we observe substantive pharmacological effects of a PYK2 inhibitor on bone resorption in OVX rats (Fig. 5*F* and Table 1). Thus, our data are not consistent with an essential role for PYK2 in osteoclast development and activity.

Table 1. Histomorphometric analysis of proximal tibia cancellous bone

Groups	Mineralizing surface, %	Mineral apposition rate, μm/day	Bone formation rate/bone surface, $\mu m^2/\mu m$ per day	Osteoclast surface, %
Sham + vehicle	24.56 ± 1.15	1.26 ± 0.06	114.15 ± 9.9	5.10 ± 0.49
OVX + vehicle	30.45 ± 2.39*	1.43 ± 0.08	163.61 ± 18.6*	8.38 ± 0.67*
OVX + EE	20.22 ± 1.40#	1.03 ± 0.06*#	77.91 ± 9.8#	4.55 ± 0.46#
OVX + PF-431396 (10)	36.81 ± 2.09*#†	1.77 ± 0.09*#†	240.17 ± 20.3*#†	7.83 ± 0.73*†
OVX + PF-431396 (30)	40.60 ± 1.77*#†	1.96 ± 0.09*#†	291.43 ± 19.1*#†	6.13 ± 0.48#

*, $P < 0.05$ vs. sham plus vehicle; #, $P < 0.05$ vs. OVX plus vehicle; †, $P < 0.05$ vs. EE.

The present body of data indicates that PYK2 plays a key role in regulating bone formation, but the detailed mechanism remains to be defined. In osteoclasts, PYK2 mediates the formation of a complex between Src and Cbl, resulting in phosphatidylinositol 3-kinase activation, but interestingly PYK2 activity appears to be dispensable (18). In contrast, *in vivo* pharmacology (Fig. 5) and hMSC culture studies using a kinase inactive mutant (Fig. 4) suggest that PYK2 activity is required to control bone formation. Src is also a negative regulator of osteogenesis (19), and like PYK2 its mechanism of action in bone formation is not well defined. Src was shown to be recruited to PYK2 and activates the enzyme through the phosphorylation of activation loop tyrosines Y-579 and Y-580 (1). Therefore, it will be important to determine whether Src and PYK2 are involved in a linear signaling pathway regulating bone formation.

Perhaps the most important finding in this article is that PYK2 inhibitors have a potential role in treating osteoporotic disease, because we observed that a PYK2 inhibitor blocks bone loss in OVX rats, an accepted preclinical model of postmenopausal bone loss. The fact that this efficacious response resulted from increased bone formation with minimal change in bone resorption has important therapeutic implications. Oral agents approved to treat osteoporosis include bisphosphonates, estrogen, and selective estrogen receptor modulators, which are antiresorptive in nature and are insufficient for restoring bone in critically osteoporotic patients. Injected human parathyroid hormone 1–34 is the only approved bone anabolic agent; however, it increases turnover with a balance favoring bone formation. Although the impact of a PYK2 inhibitor on B cell/macrophage responses needs to be considered, a small-molecule PYK2 inhibitor does represent an attractive anabolic therapy for patients afflicted by low bone mass and offers a new opportunity to impact this unmet medical need in the aging population.

Methods

Animals and Bone Analyses. All animal studies conformed with Pfizer Inc. Animal Care and Use approved protocols in accordance with the Institute of Laboratory and Animal Research guide for the care and use of laboratory animals. Generation of the PYK2−/− mice has been described (3, 15). Sprague–Dawley female rats (Taconic, Germantown, NY) were used for the PYK2 pharmacology studies. Rats were sham-operated or ovariectomized at 4.5–5 months of age. Beginning the day after surgery, animals were dosed every day by oral gavage with either vehicle (20% β-cyclodextrin in water) or the PYK2 inhibitor (PF-431396) at 10 or 30 mg/kg in vehicle for 28 consecutive days.

Peripheral Quantitative Computerized Tomography (Rat). Excised femurs were scanned with a pQCT x-ray machine (Stratec XCT Research M; Orthometrix, White Plains, NY) with software version 5.40. A 0.5-mm-thick cross section was taken at 5.0 mm proximal from the distal end with 0.10-mm voxel size. Bone area and volumetric bone content and density were determined and analyzed by using parameters previously described (20).

Bone Histomorphometry. Tibiae from rats or femora from mice were removed, dissected free of muscle, and fixed in 10% neutral buffered formalin for 24 h. Bones were then dehydrated through graded concentrations of ethanol, rinsed in xylene, and embedded in methyl methacrylate. Longitudinal sections were cut by using a Reichert-Jung Polycut S microtome at 4 and 10 μm thickness. The 10-μm sections were used unstained for dynamic histomorphometry, and the 4-μm section was stained with modified Masson's trichrome for static parameters. Measurements were made on cancellous bone using a video image analysis system (software version 2.2; Osteometrics, Atlanta, GA) as described (21).

Serum Biomarker CTX. Serum samples were collected during necropsy and stored at −20°C until analysis. C-telopeptide degradation product from type I collagen was measured by using a Ratlaps ELISA kit (Nordic Bioscience, Herlev, Denmark).

Synthesis of PF-431396. The synthesis of CF_3-pyrimidine inhibitors like PF-431396 has been described (22), and the HCl salt was used in all experiments, except for the crystal structure, which was determined with the free base (see *SI Methods* and Table 2–6).

Analysis of hMSC Cultures. hMSCs, growth medium, and osteogenic differentiation medium were obtained from Cambrex (East Rutherford, NJ). Cells were plated in growth media at a density of 3.1×10^3 cells per square centimeter in 12-well tissue culture plates and infected with adenovirus (multiplicity of infection = 400) and then changed to osteogenic induction medium (Cambrex). Alkaline phosphatase activity was measured from cell lysates on day 10 by spectrophotometrically determining conversion of *p*-nitrophenyl phosphate (Sigma, St. Louis, MO) to *p*-nitrophenol and normalized to cellular protein content by using detergent compatible Bradford reagent (Pierce, Rockford, IL). Mineralization of hMSC cultures was assessed by adding media containing 25 μg/ml calcein blue (Sigma) 48 h before fixation with cold methanol. Quantitative image analysis was performed on the ArrayScan 3.5 (Cellomics, Pittsburgh, PA); see *SI Methods* for details. Equal amounts of protein sample were run on gradient SDS polyacrylamide gels and transferred to nitrocellulose membranes. Western blots were codeveloped with monoclonal antibodies to PYK2 (BD Bioscience, San Jose, CA) and GAPDH (Advanced Immunochemical, Long Beach, CA), followed with HRP-conjugated goat anti-mouse secondary antibodies (Jackson ImmunoResearch, West Grove, PA) and chemiluminescent substrate (Pierce). Images were captured and quantitated by using Fuji Imaging Technology and Fuji Image Gauge version 4.0 software (FujiFilm USA, Stamford, CT).

Adenovirus. Infectious adenovirus particles were generated by *in vivo* recombination of plasmids containing full-length hematopoietic specific isoform WT PYK2 [amino acids 1–969 (23)], C-terminal nonkinase PYK2 [PRNK, amino acids 781-1009 (17)], kinase dead mutant PYK2 (KD, K457A), a PYK2-specific short-hairpin RNA (PYK2 SH, nucleotides 1292–1311, accession no. HSU33284), and GFP, with plasmid pVQAdCMV followed by viral amplification (ViraQuest, North Liberty, IA). Titered adenovirus stock diluted into Ultraculture medium (Cambrex) containing 2% FBS (Invitrogen, Carlsbad, CA) was used to infect hMSCs in triplicate for 4 h followed by supplementation with growth medium. After 24 h adenovirus-containing medium was replaced with osteogenic induction medium, which was changed every 2–3 days.

Bone Marrow Cultures and Analysis. Isolation and culture of mouse bone marrow have been described (24). For osteoclastic differentiation, bone marrow cells from 4-month-old mice (n = 10, each genotype) were plated into dishes or onto calcium phosphate-coated discs (BD Biosciences, Bedford, MA) at 1×10^5 cells per square centimeter in 24-well plates in complete media (phenol red-free MEMα with 15% FBS and 50 μg/ml gentamicin) containing 25 ng/ml each of osteoprotegerin ligand and macrophage colony-stimulating factor (R & D Systems, Minneapolis, MN) and cultured in 5% CO_2 at 37°C. The marrow cultures were stained for TRAP by using a leukocyte acid phosphatase kit (Sigma) on days 4, 5, and 6, and TRAP-positive cells having at least three nuclei were counted as osteoclasts. For analysis of resorption pit formation, cells growing on the calcium phosphate-coated discs were lysed in 6% bleach, rinsed with distilled water, and air-dried. Resorption pit area was

quantitated by using ImagePro Plus (Media Cybernetics, Silver Spring, MD).

For osteoblastic differentiation, cells from individual animals were plated at 1.7×10^5 cells per square centimeter in either six-well dishes (for alkaline phosphatase activity; $n = 6$ wells for each of eight mice of each genotype) or 100-mm dishes (for analysis of mineralization; $n = 4$ dishes for each of eight mice of each genotype) in growth medium (MEMα with 15% FBS). Cells were fed on days 4 and 7 with growth media and then every third day after with differentiation medium [MEMα with 10% FBS, 50 μg/ml L-ascorbic acid, 2 mM sodium phosphate (pH 7.4), and 10^{-8} M dexamethasone]. Alkaline phosphatase activity was measured on days 15 and 19 (as above). For analysis of mineralized nodule area, the cultures were fed with differentiation media supplemented with calcein blue (25 μg/ml) on day 19 and, on day 22, fixed for 10 min in 100% methanol and air-dried (see *SI Methods* for details on quantitation of bone nodule area).

Statistical Methods. StatView 4.0 (Abacus Concepts, Berkeley, CA) was used for ANOVA followed by Fisher's protected least significant difference to compare differences between groups used in the analyses of *in vivo* data. Prism 4.0 (GraphPad, San Diego, CA) or LabStats version 5 (codeveloped by Pfizer and Tessella, Abingdon, U.K.) were used in all other analyses, as described in the figure legends.

We thank J. Boer, J. Lin, and J. Houser (Pfizer, Inc., Groton, CT) for PF-431396 PK analysis; A. J. Milici (Pfizer, Inc., Groton, CT) for assistance with image analysis of osteoclast resorption pits; K. Haskell and T. Furey (Pfizer, Inc., Groton, CT and University of Connecticut, Storrs, CT) for enabling hMSC work; E. Ung and P. Whalen (Pfizer, Inc., Groton, CT) for assistance with kinase assays; J. Bordner and I. Samardjev (Pfizer, Inc., Groton, CT) for crystal structure measurements; and X. Y. Tian, X. Q. Liu, and W. S. S. Jee (University of Utah School of Medicine, Salt Lake City, UT) for performing mouse histomorphometric measurements.

1. Schlaepfer DD, Hauck CR, Sieg DJ (1999) *Prog Biophys Mol Biol* 71:435–478.
2. Guinamard R, Okigaki M, Schlessinger J, Ravetch JV (2000) *Nat Immunol* 1:31–36.
3. Okigaki M, Davis C, Falasca M, Harroch S, Felsenfeld DP, Sheetz MP, Schlessinger J (2003) *Proc Natl Acad Sci USA* 100:10740–10745.
4. Duong LT, Lakkakorpi PT, Nakamura I, Machwate M, Nagy RM, Rodan GA (1998) *J Clin Invest* 102:881–892.
5. Lakkakorpi PT, Nakamura I, Nagy RM, Parsons JT, Rodan GA, Duong LT (1999) *J Biol Chem* 274:4900–4907.
6. Sanjay A, Houghton A, Neff L, DiDomenico E, Bardelay C, Antoine E, Levy J, Gailit J, Bowtell D, Horne WC, Baron R (2001) *J Cell Biol* 152:181–195.
7. Wang Q, Xie Y, Du QS, Wu XJ, Feng X, Mei L, McDonald JM, Xiong WC (2003) *J Cell Biol* 160:565–575.
8. Pfaff M, Jurdic P (2001) *J Cell Sci* 114:2775–2786.
9. Duong LT, Nakamura I, Lakkakorpi PT, Lipfert L, Bett AJ, Rodan GA (2001) *J Biol Chem* 276:7484–7492.
10. Lakkakorpi PT, Bett AJ, Lipfert L, Rodan GA, Duong LT (2003) *J Biol Chem* 278:11502–11512.
11. Jeschke M, Standke GJ, Scaronuscarona M (1998) *J Biol Chem* 273:11354–11361.
12. Freitas F, Jeschke M, Majstorovic I, Mueller DR, Schindler P, Voshol H, Van OJ, Susa M (2002) *Bone* 30:99–108.
13. Boutahar N, Guignandon A, Vico L, Lafage PMH (2004) *J Biol Chem* 279:30588–30599.
14. Guignandon A, Boutahar N, Rattner A, Vico L, Lafage PMH (2006) *Biochem Biophys Res Commun* 343:407–414.
15. Yu Y, Ross SA, Halseth AE, Hollenback PW, Hill RJ, Gulve EA, Bond BR (2005) *Biochem Biophys Res Commun* 334:1085–1091.
16. Xiong W, Parsons JT (1997) *J Cell Biol* 139:529–539.
17. Xiong WC, Macklem M, Parsons JT (1998) *J Cell Sci* 111:1981–1991.
18. Miyazaki T, Sanjay A, Neff L, Tanaka S, Horne WC, Baron R (2004) *J Biol Chem* 279:17660–17666.
19. Marzia M, Sims NA, Voit S, Migliaccio S, Taranta A, Bernardini S, Faraggiana T, Yoneda T, Mundy GR, Boyce BF, *et al.* (2000) *J Cell Biol* 151:311–320.
20. Ke HZ, Qi H, Chidsey-Frink KL, Crawford DT, Thompson DD (2001) *J Bone Miner Res* 16:765–773.
21. Ke HZ, Brown TA, Qi H, Crawford DT, Simmons HA, Petersen DN, Allen MR, McNeish JD, Thompson DD (2002) *J Musculoskel Neuron Interact* 2:479–488.
22. Kath JC, Richter DT, Luzzio MJ (2005) Int Patent Appl WO/05023780.
23. Li X, Hunter D, Morris J, Haskill JS, Earp HS (1998) *J Biol Chem* 273:9361–9364.
24. Grasser WA, Pan LC, Thompson DD, Paralkar VM (1997) *J Cell Biochem* 65:159–171.